Published in final edited form as:
J Org Chem. 2009 December 18; 74(24): 9475–9485. doi:10.1021/jo902109u.

Site-specific Installation and Study of Electroactive Units in Every Layer of Dendrons

Malar A. Azagarsamy, **Kothandam Krishnamoorthy**, **Kulandaivelu Sivanandan**, and **S. Thayumanavan**
Department of Chemistry, University of Massachusetts, Amherst MA 01003

Abstract

While encapsulation of functional groups at the core of dendrimers is well-understood, very little is known about their intermediate layers or even the periphery. Here we report on a systematic investigation of every layer of dendrimers by incorporating a single ferrocene unit in well-defined locations in dendrons. Site-specific incorporation of the ferrocene unit was achieved utilizing the dendrimer sequencing methodology. We show here that the redox potential values of ferrocene at intermediate layers were remarkably different from that at the core and the periphery. While redox potential values were location-dependent, no significant change in the rate of heterogeneous electron transfer (k_0) was observed with respect to locations. This was attributed to the possibility that free rotation of dendrimer nullifies the distance between the electrode and ferrocene unit. Finally, we also show that no Faradaic current was observed for the amphiphilic assemblies of these dendrons, while the same dendron did exhibit significant Faradaic current in non-assembling solvent environments.

Introduction

Dendrimers, despite their complexities, are attractive macromolecular architectures as they can be obtained with well-defined molecular weights and precise number of functional groups.[1] Since dendrimers become globular at higher molecular weights, there have been an interest in functionalizing them with photo-, electro- and catalytically active units for a variety of applications.[2-4], Generally, these active units are incorporated either at the core, where there is significant encapsulation and protection from the environment, or at the periphery of dendrimers, where opportunity exists for loading a large number of functional moieties.[2-6] While there have been comparisons between the solvent-exposed peripheral functionalities and the well-encapsulated core functional groups, very little is known about the intermediate layers in these molecules. Therefore, the microenvironment variations from the core to the periphery of the dendrimers are not well understood.

Note that significant amount of work has been previously reported on the encapsulation of electroactive functionalities using dendritic scaffolds.[2-6] These works have specifically focused on understanding features such as the effect of generational variations in dendrimers and the nature of dendrimer backbones upon the encapsulation efficiency of electroactive scaffolds incorporated at the core or focal points of dendritic architectures. Our work here is focused on understanding the change in encapsulation of an electroactive functionality at the periphery, focal point, and the intermediate layers of dendrons. One of the issues in comparing different locations of a dendrimer involves the variation in number density of the functional moieties in different layers. For example, in a third generation monodendron, the number of

thai@chem.umass.edu.

Supporting Information Available: experimental details. This material is available free of charge at http://pubs.acs.org.

identical functional groups in the periphery would be eight compared to a single focal point moiety. There is a progressive variation in this number in the intermediate layers. This variation significantly complicates the meaningful comparisons regarding the microenvironment of different locations. An unambiguous way to address this issue would be to incorporate a single active functional group at a predetermined location of the dendrimer. To be successful in such a venture, it is necessary that we access synthetic methods that allow variations in the two Bs of an AB_2 monomer. In a preliminary communication,[7] we had incorporated a photoactive anthracene moiety at precise locations within benzyl ether dendrons using the synthetic methods we had developed previously.[8] In that report, we utilized Stern-Volmer quenching to probe the access of guest molecules to various locations within dendrimers, where we observed a precipitous change in the guest access at the intermediate layers of the dendrimers. While those findings provide insights in homogeneous solutions, it is invaluable to also understand the accessibility of functional groups in dendrimers in the context of heterogeneous electron transfer, since this provides more direct information on encapsulation and dendritic shielding effects. Here, we report on the design, syntheses, and the electrochemical investigation of dendrons with a single ferrocene unit at different locations.

Results and Discussion

Molecular design and synthesis

We chose to incorporate ferrocene as the electroactive unit within these dendrons, since its electrochemical behavior is well understood.[5,6,9] We have utilized our recently reported biaryl dendrimers as the scaffold, because of the additional phenyl ring, which provides a handle to incorporate electroactive functionalities (*i.e.* in addition to the AB_2 functionalities necessary for the dendritic growth).[10] The biaryl dendrimers contain a carboxylic ester functionality in one face and a decyl moiety on the other side in each of the repeat units within the dendron.[10a] To install a single ferrocene unit at specific locations, one of the decyl units was replaced with a ferrocene unit. The structures of dendrons upto third generation are shown in Chart 1. It is important to reiterate that within these structures, there is only one ferrocene unit at any one time. For example, in a G3 dendron, when the peripheral layer contains a ferrocene unit (R_4 = Fc derivative), all other R groups in the structure are decyl moieties (R_1-R_3 = *n*-$C_{10}H_{21}$). To easily follow the structures of the dendrons during our discussion, we have used the following naming scheme. We have assigned the focal point of the dendron as the first layer L1. Thus, for a G3 dendron, the focal point functionalization would be **G3(L1)**, while the functionalization at the periphery would correspond to **G3(L4)** (see Chart 1).

Although the structures targeted here are focused on incorporation of ferrocene, we envisaged that it is useful to have a general synthetic strategy that allows for functionalizing the dendrimer with versatile active units at desired locations. Therefore, we were interested in a modular synthetic scheme, where the ferrocene unit is incorporated in the final stage of the synthesis. For this purpose, incorporation of a single reactive functionality that can tolerate the reaction conditions used in the syntheses of biaryl dendrimers is described. We have chosen an alkyne unit as the reactive functionality so that any desired active unit can be incorporated easily through the copper catalyzed Huisgen 1,3-dipolar cycloaddition, which is popularly known as “click” chemistry.[11]

Incorporation of a single functional unit at the periphery of a dendron is more challenging than that at the focal point. This is because the focal point has only one location for functionalization, whereas there are multiple identical locations in the periphery. For example, the G3 dendron (Chart 1) contains eight identical peripheral units; here the challenge resides in functionalizing only one of them. To achieve this, we utilized our dendrimer sequencing methodology that is based on protection-deprotection strategies.[8b,8c] Since our dendrons are based on AB_2 biaryl repeating unit **1** (Chart 2),[10a] it is necessary to differentiate the two B functionalities in order

to introduce sequences within the dendrimer. To execute this, one of the B functionalities of AB_2 should be protected and thus the targeted monomer is designated as ABB_p **2** (Chart 2). After reacting the unprotected B functionality with one equivalent of A, the protected B will be liberated and then reacted with a different monomer. This allows for the incorporation of two different A's on to an AB_2 building block. Based on this approach for the synthesis of precisely functionalized dendrons (Chart 1), the main building blocks required are the AB_2 biaryl unit **1**, and the ABB_p unit **2**, and the peripheral unit **G0(L)**.

The syntheses of the building blocks **1** and **2** started with *tert*-butyldimethylsilyl (TBS) protected aryl stannane **3** and 3,5-dihydroxy bromobenzoic acid **4**, following our previous reports to obtain the biaryl aldehyde **5**.[10a] Deprotection of TBS groups followed by the reduction of aldehyde provided the AB_2 monomer **1**. The bottleneck here involved the mono protection of AB_2 monomer **1**. Our initial trials to mono protect **1** using MOM-Cl in the presence of K_2CO_3 had resulted in the hydrolysis of *t*-butyl ester. When Hunig's base was used instead of K_2CO_3, there was no selectivity towards the phenolic hydroxyl group over the primary aliphatic hydroxyl group. Finally, the mono-protection was achieved on the biaryl aldehyde **6** thereby avoiding the presence of the primary aliphatic hydroxyl group during the protection step. The final reduction on the mono protected aldehyde yielded the monomer ABB_p **2** (Scheme 1).

The periphery **G0(L)** containing alkyne moiety was synthesized by first mono alkylating 3,5-dihydroxy benzyl alcohol (**7**) with *t*-butylbromoacetate in the presence of potassium carbonate and 18-crown-6 (Scheme 2). The mono alkylated compound was further treated with 1-bromo-4-pentyne to afford **G0(L)**. The resultant hydroxymethyl compound **G0(L)** was converted to its bromide **8** using a CBr_4/PPh_3 combination. Along with these building blocks, we also require the bromides of symmetrical dendrons **G0-Br**, **G1-Br** and **G2-Br** (Chart 3), which were synthesized following our earlier report.[10a]

The first generation dendron **G1(L2)** (Chart 1) was synthesized by sequentially introducing two different peripheral units. The monomer **1** was first treated with a stoichiometric amount of **G0-Br** to get mono-substituted compound **9**, which was further treated with bromide **8** to obtain **G1(L2)** (Scheme 3). Note that here we did not utilize our protection-deprotection strategy, because of the easy separation of mono-substituted compound from a mixture of products. However, the separation was cumbersome in the case of the second and third generation dendrons. Thus we have decided to use the mono-protected ABB_p monomer **2**. To synthesize the second generation **G2(L3)**, monomer **2** was treated with symmetrical **G1-Br** in the presence of K_2CO_3 and the resultant compound was subjected to MOM-deprotection to afford the compound **10**. The phenolic compound **10** was then treated with **11**, obtained by the bromination of **G1(L2)**, to provide **G2(L3)** dendron. Similarly, treating the ABB_p monomer **2** with **G2-Br** followed by the deprotection of MOM afforded the compound **12**, which was further treated with **13** to yield **G3(L4)** dendron as shown in Scheme 3.

Synthesis of dendrons with the functionality at the focal point is relatively straightforward, except that it requires a central core unit **14** that contains an alkyne moiety. The synthesis of core unit **14** is outlined in Scheme 4. The key step in the synthesis of this unit is the Stille coupling between the MOM-protected aryl stannane **15** and aldehyde **16**. The aryl stannane **15** was obtained from commercially available 1-bromo-3,5-dimethoxybenzene **17** in three steps. The steps involve the deprotection of methyl groups followed by the protection of free hydroxyl groups using MOM-Cl. The resultant MOM-protected bromobenzene was treated with *n*-BuLi, followed by tributyltin chloride to obtain the aryl stannane **15**. On the other hand, the bottom ring **16** was obtained from 4-bromo-3,5-dihydroxybenzoic acid **4**, which was first converted to the corresponding benzyl alcohol, 4-bromo-3,5-dihydroxybenzyl alcohol (Scheme 4). This molecule was first treated with one equivalent of *t*-butyl bromoacetate to

isolate the mono-substituted product. The product was then subjected to PCC oxidation to yield the aldehyde **16**. The 4-bromobenzaldehyde **16** and aryl stannane **15** were then subjected to the palladium (II) catalyzed Stille coupling reaction to achieve the biaryl compound. The biaryl compound was further treated, with 1-bromo-4-pentyne followed by the reduction of the aldehyde and the final deprotection of the MOM groups, yielding the monomer **14**. The core functionalized 1st generation **G1(L1)** was synthesized by treating monomer **14** with two equivalents of **G0-Br** as shown in Scheme 5. Similarly, the second and third generation dendrons, **G2(L1)** and **G3(L1)**, were obtained by treating monomer **14** with **G1-Br** and **G2-Br** respectively (Scheme 5).

Functionalizing the intermediate layers also requires the sequencing methodology. It is important to note that the G2 dendron has only one intermediate layer, where as the G3 dendron has two intermediate layers. Thus totally three different dendrons **G2(L2), G3(L2)** and **G3 (L3)** had to be synthesized. As shown in Scheme 6, the synthesis of **G2(L2)** was accomplished by first converting the core functionalized lower generation **G1(L1)** to its bromide using a CBr_4/PPh_3 combination and then treating the bromide with compound **10**. Similarly, other dendrons **G3(L2)** and **G3(L3)** were synthesized by bromination of corresponding 2nd generation dendrons and subsequent treatment with compound **12** (Scheme 6).

After the site-specific incorporation of the acetylene moiety into the dendrons, we moved on to install the ferrocene unit through click chemistry. Treatment of these acetylene-containing dendrons with azidomethyl ferrocene in the presence of a catalytic amount of copper sulphate and sodium ascorbate afforded the corresponding triazole derivatives as exemplified in Scheme 7. Structures of these ferrocene-incorporated dendrons are shown in Chart 1. All these dendrimers were characterized using ^{1}H NMR, ^{13}C NMR and matrix-assisted laser-desorption time of flight (MALDI-ToF) mass spectrometry.[12]

Electrochemical Studies

The electrochemical properties of the ferrocene-incorporated dendrons were investigated using cyclic voltammetry. Cyclic voltammograms (CV) were recorded in DMF using 10 μm platinum disk as the working electrode, Pt wire as counter electrode, and Ag/Ag^+ as reference electrode. [12] All dendrons showed the s-shaped steady state CV (see Figure 1 for example) anticipated in microelectrode-based experiments. The redox potentials ($E_{1/2}$) obtained for the ferrocene unit in these dendrons are shown in Table 1. In all these cases, the non-dendron molecule **G0** could be considered as the control, which exhibited an $E_{1/2}$ of about 103 mV. The two layers in the lowest generation dendrons, **G1**, did not show any significant difference in the redox potential of the ferrocene unit (118 mV for the focal point and 114 mV for the peripheral layer). However, the relative $E_{1/2}$ values of the **G2** and **G3** dendrons were interesting. In the case of **G2**, the redox potentials of the focal point and the peripheral layer were similar to those observed with **G1**. However, the $E_{1/2}$ of the ferrocene functionality placed at the intermediate layer in this dendron was found to be 69 mV, compared to 113 mV and 117 mV for the focal point and the peripheral ferrocenes respectively. A similar trend was also observed with the **G3** dendron. In this generation, the ferrocene unit could be incorporated in four different locations, as there are two intermediate layers. Once again, the redox potential of the ferrocene incorporated at the intermediate layer was found to be about 40-60 mV different from those observed with the focal point and peripheral functional groups (see Table 1). The $E_{1/2}$ values of the ferrocene at the intermediate layers were found to be 60 and 68 mV, compared to 101 and 120 mV for the focal point and peripheral ferrocenes respectively. Difference in $E_{1/2}$ value is related to the thermodynamic stability differences between the reduced and the oxidized state of the electroactive molecule. The lower redox potentials, observed for an otherwise identical ferrocene unit at the intermediate layers, suggest that the ferrocenium ion product is more stabilized in these intermediate layers compared to the peripheral functionality. These could

be taken to suggest that the ferrocene units located in the intermediate layers are less solvent-exposed compared to the focal point and the periphery. It is also likely that the ferrocenium (Fe^{3+}) ion is better stabilized by the dendrimer backbone compared to DMF. This is an interesting observation with dendrons. Conventional wisdom about dendrons and dendrimers suggest that the focal point or core of these molecules provide significantly different microenvironments, compared to the periphery. With these studies, we clearly show that it is the intermediate layers that behave significantly differently from the focal point and periphery of the dendrons. A question is: why not interpret these results to suggest that the ferrocenes at the intermediate layers are more exposed to the solvent, because the periphery is more crowded (sterically) and the core is encapsulated and the ferrocene unit? The fact that the $E_{1/2}$ value in lower generation dendrons, where the ferrocene unit is clearly more solvent-exposed, are closer to the peripheral and focal point $E_{1/2}$ values in higher generation dendrons supports our explanation that the dendrimer backbone indeed facilitates the oxidation of ferrocene units in the intermediate layers of the dendrons.

In order to visualize these dendrons, we obtained the energy-minimized structures of G3 dendron using MM2 (Figure 2). Interestingly, ferrocene functionality was enclosed by the biaryl backbone in case of **G3(L2)Fc** dendron that contain ferrocene in the intermediate layer, while it was placed out of the dendrimer backbone in dendrons that contain ferrocene unit at the core and periphery. However in contrast to our interpretation, the ferrocene placed in the other intermediate layer of **G3(L3)Fc** dendron, seems to be still presented at edge of dendrimer backbone. Note that these structures are obtained by energy minimization in the gas phase and thus do not account for the differential solvation of substituents. We suggest this as the reason for the observed discrepancy.

Considering the differences in the thermodynamics of the redox active species in different layers, we were also interested in investigating the kinetics of the heterogeneous electron transfer reactions. As a first step towards the calculation of kinetic parameters, the diffusion coefficient (D_0) was calculated utilizing the limiting current obtained from the steady state CV for each of the generation. We had assumed that within a generation the D_0 would be identical and thus the estimation of D_0 was achieved using the more abundantly available focal point functionalized dendrons of each generation. As shown in Table 1, the D_0 decreases upon increase in generation number, which is the general trend observed for dendrimers. The obtained D_0 values were utilized to calculate the standard rate constants for heterogeneous electron transfer (k^0).[13,5i]

While the D_o values were found to follow the general trend, the k^0 values did not vary significantly as a function of generation number or the location of the ferrocene (Table 1). All rate constant values were found to be about 1-2 × 10^{-4} cm/s. Similar k^0 values for the first and second-generation dendrons is perhaps not surprising (we do not have an explanation for the slightly higher k^0 for **G1(L2)Fc**). However, the insignificant changes in k^0 of ferrocenes in various layers of higher generation dendrons are surprising. This is possibly due to the free rotation of the dendrons that leads to an orientation in which the ferrocene is conveniently accessed by the electrode irrespective of its location. For example, in the case of **G3(L1)Fc** and **G3(L4)Fc**, the ferrocene is at the core and at the periphery of the dendron respectively. It is reasonable that the dendrons could rotate rapidly near the electrode surface. Therefore, it is easy to imagine that the rotation of the dendron leads to an orientation in which the ferrocene is equidistant from the electrode in both **G3(L1)Fc** and **G3(L4)Fc** as illustrated in Figure 3. Such orientations result in similar k^0 values for both **G3(L1)Fc** and **G3(L4)Fc**. The energy minimized structures in Figure 2 further supports this hypothesis. Similarly, ferrocene in **G3 (L2)Fc** and**G3(L3)Fc** are only one layer away from **G3(L1)** and **G3(L4)** respectively. Hence, it is possible that the k^0 value is essentially unchanged. These results show that the dendrimer

growth does not effectively shield the ferrocene unit from the electrode, although the ferrocenium ion product is stabilized differently in various layers of the dendrons.

Finally, we were interested in studying the electrochemical behavior of these ferrocene units in amphiphilic supramolecular assemblies that could be obtained from these dendrons. An interesting feature about the biaryl-based dendrons is that the hydrolysis of the *tert*-butyl esters would provide the facially amphiphilic dendrons shown in Chart 4.[12] We have previously shown that these dendrons provide unique environment-dependent assemblies.[10a] Therefore, the carboxylic ester functional groups in the ferrocene containing dendrons above were hydrolyzed.[14] To study the electrochemical behavior of the ferrocene units incorporated within these amphiphilic dendrons, these molecules were first dissolved in water at a concentration above their respective critical aggregation concentrations (CACs) to form the micellar assemblies.

The electrochemical studies of these assemblies were then performed using the platinum microelectrode as the working electrode. We were surprised to find that there was no discernible CV from these dendrons (Figure 4a). The behavior was found to be rather capacitive in nature. This observation could be due to one of the two following reasons: (*i*) ferrocene has detached from the dendron or became electro-inactive during the ester hydrolysis and work up; (*ii*) ferrocene is buried in the hydrophobic pocket of these rather large micellar assemblies (~40-100 nm). To distinguish these possibilities, we recorded the CV of the hydrolyzed dendron in DMF. Dynamic light scattering (DLS) studies of these dendrons have confirmed that these amphiphilic dendrons do not aggregate in DMF, since the solvent is compatible with both the carboxylic acid and the decyl functionalities. Therefore, we should observe a steady state CV if the ferrocene is intact and electro-active. Indeed, we did observe a steady state CV for the hydrolyzed dendron, which confirms that the ferrocene is indeed electro-active and intact (Figure 4b).

It is also interesting to note that while there was no significant faradaic current from the micellar assemblies of all the amphiphilic dendrons, the small molecule surfactant **G0(L)Fc-COOH** displayed a steady state CV. A possible explanation for this is that, in the case of small molecule surfactant **G0(L)Fc-COOH**, there exists a significant amount of free monomeric surfactant in solution due to the rather fast equilibrium between the small molecule and the micellar assembly. As a result, the ferrocene would be easily available for electron transfer in the monomeric surfactants, accounting for the observed voltammetric response. On the other hand, the dendrons form more tightly packed assemblies due to the covalent linking of the monomeric units. Thus, the concentration of monomeric dendritic units would be too low in solution to be observable. Similar observations, in which no significant electron transfer was seen when ferrocene was encapsulated in a hydrophobic host, were reported recently.[10] Nonetheless, these results show that the amphiphilic assemblies provides an interesting pathway for fully silencing an electroactive unit, which can then be released to become electroactive in an alternate environment, *i.e.* from water-like to DMF-like environment.

Experimental Section

General procedure for introducing ferrocene unit using “Click” chemistry

To a solution of alkyne-functionalized dendrimers (1.0 equiv.) in THF/DMF/H_2O (1:1:1), azidomethyl ferrocene (4.0-8.0 equiv.), $CuSO_4$ (0.1 equiv.) and sodium ascorbate (0.1 equiv.) was added. The reaction mixture was heated at 50 °C for 12 hours. Progress of the reaction was monitored by thin layer chromatography (TLC). After completion of the reaction, the reaction mixture was partitioned between ethyl acetate and saturated NH_4Cl solution. The aqueous layer was extracted twice with ethyl acetate and the combined organic layer was dried

over anhydrous Na_2SO_4 and evaporated to dryness. The crude product was isolated by silica gel column chromatography.

Synthesis of G0(L)Fc

According to the general procedure for click chemistry, **G0(L)** (0.1 g, 0.31 mmol) was treated with azidomethyl ferrocene (4 eq.) to yield 0.14 g (80%) of **G0(L)Fc**. ^{1}H NMR (400 MHz, $CDCl_3$) δ 7.19 (s, 1H), 6.51 (s, 1H), 6.47 (s, 1H), 6.34 (t, *J* =2.4 Hz, 1H), 5.22 (s, 2H), 4.58 (d, *J* =4.0 Hz, 2H), 4.46 (s, 2H), 4.24 (t, *J* = 1.6 Hz, 2H), 4.19-4.16 (m, 7H), 3.92 (t, *J* = 6.0 Hz, 2H), 2.81 (t, *J* = 7.2 Hz, 2H), 2,43, (bs, 1H), 2.12-2.05 (m, 2H), 1.47 (s, 9H); ^{13}C NMR (100 MHz, $CDCl_3$) δ 168.0, 160.2, 159.1, 147.0, 143.7, 120.4, 106.1, 104.9, 100.7, 82.4, 81.1, 77.4, 77.3, 77.1, 76.8, 69.0, 68.9, 66.9, 65.7, 65.0, 49.9, 28.8, 28.1, 22.1; FAB/MS *m/z* (r.i.) 561 (M^+, 40), 362(15), 307(20), 199(100). HRMS (FAB+) calculated for $C_{29}H_{35}FeN_3O_5$ 561.1927, found 561.1942.

Synthesis of G1(L2)Fc

The alcohol **G1(L2)** (0.05 g, 0.08 mmol) was subjected to click reaction as per the general procedure to yield 0.055 g (92%) of **G1(L2)Fc**. ^{1}H NMR (400 MHz, $CDCl_3$) δ 7.50 (s, 1H), 6.96-6.40 (m, 11H), 5.33-5.22 (m, 2H), 4.92 (s, 4H), 4.66 (s, 2H), 4.47-4.41 (m, 7H), 4.30-4.10 (m, 8H), 3.90 (m, 6H), 2.84 (bs, 2H), 2.29-1.18(m, 61H), 0.88-0.81 (m, 6H); ^{13}C NMR (100 MHz, $CDCl_3$) δ 168.0, 167.8, 160.3, 160.0, 159.0, 156.9, 155.8, 147.0, 141.8, 139.5, 135.5, 119.2, 110.1, 107.0, 105.4, 105.3, 104.8, 103.5, 101.0, 100.7, 82.2, 82.0, 69.9, 69.5, 68.7, 68.0, 66.8, 66.2, 65.7, 65.3, 49.6, 31.8, 29.5, 29.4, 29.3, 29.2, 29.1, 28.9, 28.0, 25.9, 22.5, 22.0, 14.0; MALDI-ToF *m/z* 1422.9, 1445.7 ($C_{81}H_{111}FeN_3O_{15}$ requires 1422.6 and $C_{81}H_{111}FeN_3O_{15}$ +Na^+ requires 1445.6).

Synthesis of G2(L3)Fc

According to the general procedure for click reaction, **G2(L3)** (0.08g, 0.3 mmol) was reacted with azidomethyl ferrocene (6.0 eq.) to yield 0.08g (93%) of **G2(L3)Fc**. ^{1}H NMR (400 MHz, $CDCl_3$) δ 7.20 (s, 1H), 6.77-6.39 (m, 27H), 5.25 (s, 2H), 5.00-4.95 (m, 12H), 4.70-4.69 (m, 2H), 4.50-4.45 (m, 14H), 4.26 (t, *J* = 1.6 Hz, 2H), 4.19-4.16 (m, 9H), 3.97-3.90 (m, 14H), 2.86 (t, *J* = 7.6 Hz, 2H), 2.15-2.13 (m, 2H) 1.92 (bs, 1H), 1.80-1.20 (m, 159H), 0.90-0.83 (m, 18H); ^{13}C NMR (100 MHz, $CDCl_3$) δ 168.0, 167.8, 160.5, 160.4, 160.2, 159.1, 157.4, 156.1, 147.0, 141.9, 139.7, 139.6, 137.9, 137.8, 135.8, 135.7, 120.4, 119.7, 119.7, 119.3, 110.2, 107.0, 105.7, 105.6, 105.4, 104.8, 104.4, 104.2, 103.5, 101.2, 101.0, 98.2, 82.3, 82.3, 82.1, 82.0, 82.0, 81.1, 70.2, 69.9, 69.0, 68.9, 68.9, 68.1, 66.9, 66.3, 66.2, 65.8, 65.4, 50.0, 32.0, 29.6, 29.4, 29.3, 29.2, 28.1, 26.1, 22.7, 22.0, 14.2; MALDI-ToF *m/z* 3143.1 ($C_{185}H_{263}FeN_3O_{35}$ requires 3144.9).

Synthesis of G3(L4)Fc

According to the general procedure for click reaction, **G3(L4)** (0.07 g, 0.011 mmol) was reacted with azidomethyl ferrocene (8.0 eq.) to yield 0.6 g (83%) of **G3(L4)Fc**. ^{1}H NMR (400 MHz, $CDCl_3$) δ 7.21 (s, 1H), 6.79-6.43 (m, 59H), 5.25 (s, 2H), 5.03-4.95 (m, 28H), 4.70-4.69 (m, 2H), 4.50-4.46 (m, 30H), 4.26 (s, 2H), 4.20-4.17 (m, 7H), 3.97-3.90 (m, 30H), 2.86 (t, *J* = 7.2 Hz, 2H), 2.15-2.13 (m, 2H) 1.80-1.15 (m, 359H), 0.90-0.83 (m, 42H); ^{13}C NMR (100 MHz, $CDCl_3$) δ 168.0, 168.0, 167.9, 167.9, 160.5, 160.2, 159.2, 159.1, 157.4, 156.1, 147.0, 141.9, 139.6, 137.9, 137.8, 135.8, 135.6, 120.3, 119.8, 119.3, 110.2, 107.0, 105.8, 104.6, 101.2, 101.0, 82.3, 82.1, 82.0, 82.0, 82.0, 81.1, 70.2, 69.9, 69.0, 68.9, 68.9, 68.1, 66.9, 66.3, 66.2, 65.7, 65.5, 49.9, 32.1, 31.9, 29.6, 29.6, 29.4, 29.3, 29.3, 29.2, 29.1, 28.8, 28.1, 26.1, 22.7, 22.2, 14.0; MALDI-ToF *m/z* 6610.9 ($C_{393}H_{567}FeN_3O_{75}$+$Na^+$ requires 6612.5).

Synthesis of G1(L1)Fc

The alcohol **G1(L1)** (0.09 g, 0.08 mmol) was subjected to click reaction as per the general procedure to yield 0.10 g (85%) of **G1(L1)Fc**. ^{1}H NMR (400 MHz, $CDCl_3$) δ 7.02 (bs, 1H), 6.70-6.39 (m, 11H), 5.08 (bs, 2H), 4.91 (s, 4H), 4.62 (s, 2H), 4.50-4.4 (m, 6H), 4.20-4.09 (m, 9H), 3.88 (t, *J* = 5.6 Hz, 6H), 2.63 (bs, 2H), 2.42 (bs, 1H), 1.97 (bs, 2H), 1.75-1.70 (m, 4H), 1.50- 1.19 (m, 55H), 0.88-0.84 (t, *J* = 6.8 Hz, 6H); ^{13}C NMR (100 MHz, $CDCl_3$) δ 167.9, 167.7, 160.3, 159.0, 159.0, 156.9, 155.8, 146.6, 142.1, 139.4, 135.7, 120.7, 118.9, 110.1, 106.8, 105.3, 104.7, 103.3, 101.0, 100.7, 82.1, 81.8, 69.7, 69.1, 67.9, 67.1, 66.0, 65.5, 65.0, 49.6, 31.7, 29.4, 29.4, 29.2, 29.1, 29.0, 28.3, 27.9, 25.8, 22.5, 21.5, 14.0; MALDI-ToF *m/z* 1423.3 and 1446.4 ($C_{81}H_{111}FeN_3O_{15}$ requires 1422.6 and $C_{81}H_{111}FeN_3O_{15} + Na^+$ requires 1446.6).

Synthesis of G2(L1)Fc

According to the general procedure for click reaction, **G2(L1)** (0.3 g, 0.10 mmol) was reacted with azidomethyl ferrocene to yield 0.31g (96%) of **G2(L1)Fc**. ^{1}H NMR (400 MHz, $CDCl_3$) δ 7.06 (bs, 1H), 6.75-6.35 (m, 27H), 5.12 (s, 2H), 5.00-4.92 (m, 12H), 4.65 (s, 2H), 4.50-4.41 (m, 14H), 4.18-4.08 (m, 9H), 3.92-3.85 (m, 14H), 2.68 (bs, 2H), 2.01-1.10 (m, 163H), 0.90-0.81 (m, 18H); ^{13}C NMR (100 MHz, $CDCl_3$) δ 167.9, 167.8, 160.3, 159.0, 159.0, 157.3, 155.9, 139.4, 137.6, 135.4, 119.6, 110.1, 106.9, 105.6, 105.3, 104.4, 101.1, 100.8, 82.2, 82.0, 81.9, 70.1, 69.8, 68.7, 68.0, 66.2, 65.6, 31.8, 29.5, 29.4, 29.3, 29.2, 29.1, 29.0, 27.9, 25.9, 22.6, 14.0; MALDI-ToF *m/z* 3168.5, 3145.6 ($C_{185}H_{263}FeN_3O_{35}$+$Na^+$ requires 3167.9 and $C_{185}H_{263}FeN_3O_{35}$ requires 3144.9).

Synthesis of G3(L1)Fc

As per the general procedure for click reaction, **G3(L1)** (0.14 g, 0.02 mmol) was reacted with azidomethyl ferrocene to yield 0.12 g (80%) of **G3(L1)Fc**. ^{1}H NMR (300 MHz, $CDCl_3$) δ 7.08 (s, 1H), 6.80-6.40 (m, 59H), 5.13 (s, 2H), 5.02-4.92 (m, 28H), 4.66 (s, 2H), 4.52-4.42 (m, 30H), 4.22-4.08 (m, 9H), 3.97-3.88 (m, 30H), 2.74-2.68 (m, 2H), 2.08-1.09 (m, 361H), 0.90-0.81 (m, 42H); ^{13}C NMR (75 MHz, $CDCl_3$) δ 167.9, 167.9, 167.8, 160.3, 159.0, 159.0, 158.9, 157.3, 157.0, 155.9, 146.6, 142.0, 139.4, 137.7, 137.6, 135.8, 135.6, 135.4, 120.4, 119.6, 119.5, 119.0, 110.0, 106.9, 105.6, 105.2, 104.7, 104.4, 103.4, 101.1, 100.8, 82.2, 82.0, 81.9, 81.9, 81.2, 70.1, 69.7, 68.8, 67.9, 67.3, 66.1, 66.0, 65.6, 65.1, 49.6, 31.7, 29.4, 29.2, 29.2, 29.1, 29.0, 28.5, 28.1, 27.9, 25.9, 22.5, 14.0; MALDI-ToF *m/z* 6587.0 ($C_{393}H_{567}FeN_3O_{75}$ requires 6589.5).

Synthesis of G2(L2)Fc

According to the general procedure for the formation of triazole, **G2(L2)** (0.12 g, 0.04 mmol) was subjected for click reaction to yield 0.10 g (75%) of **G2(L2)Fc**. ^{1}H NMR (300 MHz, $CDCl_3$) δ 7.00 (s, 1H), 6.78-6.39 (m, 27H), 5.08 (s, 2H), 5.00-4.91 (m, 12H), 4.68 (s, 2H), 4.49-4.41 (m, 14H), 4.19-4.08 (m, 9H), 3.95-3.85 (m, 14H), 2.65-2.58 (m, 2H), 1.97-1.15 (m, 163H), 0.90-0.78 (m, 18H); ^{13}C NMR (75 MHz, $CDCl_3$) δ 167.9, 167.9, 167.8, 167.8, 167.7, 160.3, 160.3, 159.0, 159.0, 158.9, 157.3, 157.2, 156.8, 155.9, 146.6, 141.9, 139.4, 139.3, 137.9, 137.6, 135.7, 135.6, 135.4, 120.6 119.5, 119.5, 119.0, 110.1, 110.0, 106.9, 105.7, 105.5, 105.3, 105.2, 104.6, 104.3, 103.3, 101.1, 100.8, 100.8, 82.2, 82.2, 81.9, 81.9, 70.0, 69.7, 68.7, 68.0, 67.9, 67.2, 66.1, 66.0, 65.6, 65.2, 31.7, 29.4, 29.4, 29.2, 29.2, 29.1, 29.0, 28.4, 27.9, 25.9, 25.8, 22.7, 22.5, 21.5, 14.0; MALDI-ToF *m/z* 3143.6, 3166.5 ($C_{185}H_{263}FeN_3O_{35}$ requires 3144.9 and $C_{185}H_{263}FeN_3O_{35}$+$Na^+$ requires 3167.9).

Synthesis of G3(L2)Fc

According to the general procedure for the formation of triazole, **G3(L2)** (0.1 g, 0.01 mmol) was reacted with azidomethyl ferrocene to yield 0.08 g (80%) **G3(L2)Fc**. ^{1}H NMR (300 MHz, $CDCl_3$) δ 7.05 (s, 1H), 6.81-6.40 (m, 59H), 5.12-4.90 (m, 30H), 4.68 (s, 2H), 4.52-4.42 (m, 30H), 4.16-4.07 (m, 9H), 3.98-3.88 (m, 30H), 2.71-2.68 (m, 2H), 2.05-1.15 (m, 361H), 0.86

(m, 42H); ^{13}C NMR (75 MHz, $CDCl_3$) δ 167.9, 167.8, 160.3, 159.0, 158.9, 157.3, 156.9, 155.9, 146.6, 141.9, 139.4, 138.0, 137.7, 137.6, 137.5, 135.7, 135.6, 135.4, 120.4, 119.6, 119.0, 110.0, 106.9, 105.6, 105.3, 104.6, 104.4, 103.2, 101.0, 100.8, 82.2, 81.9, 81.9, 81.1, 70.0, 69.7, 68.7, 68.4, 67.9, 67.3, 66.1, 65.6, 65.2, 60.5, 31.7, 29.4, 29.2, 29.2, 29.1, 29.0, 28.5, 27.9, 25.9, 22.5, 14.0; MALDI-ToF *m/z* 6612.8, 6588.8 ($C_{393}H_{567}FeN_3O_{75}$+Na requires 6612.5 and $C_{393}H_{567}FeN_3O_{75}$ requires 6589.5).

Synthesis of G3(L3)Fc

According to the general procedure for click reaction, **G3(L3)** (0.11 g, 0.018 mmol) was reacted with azidomethyl ferrocene to yield 0.08 g (74%) of **G3(L3)Fc**. ^{1}H NMR (300 MHz, $CDCl_3$) δ 7.01 (s, 1H), 6.79- 6.40 (m, 59H), 5.10 (s, 2H), 5.02- 4.88 (m, 28H), 4.68 (s, 2H), 4.50-4.41 (m, 30H), 4.25- 4.05 (m, 9H), 3.97-3.84 (m, 30H), 2.68-2.62 (m, 2H), 2.00-1.90 (m, 361H), 0.90-0.75 (m, 42H); ^{13}C NMR (75 MHz, $CDCl_3$) δ 167.9, 167.8, 167.8, 167.7, 160.3, 159.0, 159.0, 158.9, 157.2, 156.9, 1559, 146.6, 141.8, 139.4, 139.3, 137.8, 137.6, 135.7, 135.6, 135.4, 120.6, 119.6, 119.5, 119.0, 110.0, 106.9, 105.6, 105.2, 104.6, 101.0, 100.8, 82.2, 81.9, 81.2, 70.0, 69.7, 68.7, 67.9, 66.1, 65.6, 31.7, 29.4, 29.4, 29.2, 29.2, 29.1, 29.0, 28.4, 27.9, 25.9, 22.5, 22.5, 14.0; MALDI-ToF *m/z* 6588.3 ($C_{393}H_{567}FeN_3O_{75}$ requires 6589.5).

Summary

Differential encapsulation of active functionalities in dendrimers has been previously studied in the context of generation dependence. Very little attention has been paid to the differences in the encapsulation of functional groups within different layers of dendrimers. We have designed, synthesized, and studied electroactive dendrons to investigate the possible variations. In our studies, we have shown that: (*i*) we could obtain dendrons where an electroactive functionality can be incorporated at specific locations in dendrons. We have utilized the dendrimer sequencing methods and the versatile 1,3-dipolar cycloaddition (click reaction) to incorporate the electroactive moiety at different layers. This chemistry also provides an opportunity to incorporate any desired functionality at a precise location in dendrimers; (*ii*) while the redox potential of ferrocene did not vary with generation, the $E_{1/2}$ values were significantly different in the intermediate layers at higher generation dendrons. These results suggest that the microenvironment of the intermediate layers is dictated by the dendron, while that of the periphery and the core is similar to the solvent. (*iii*) although there are thermodynamic variations, there are no discernible differences in the kinetics of the heterogeneous electron transfer processes in various layers of the dendrons. (*iv*) the self-assembled amphiphilic assembly versions of these dendrons do not exhibit any CV signals in aqueous solutions. We attribute to this to the burial of the electroactive functionality in the amphiphilic assembly, because when studied in a solvent where the dendron does not self-assemble, the electroactive functionality becomes very much accessible. These results suggest that our amphiphilic dendron assemblies could be used to provide environment-dependent protection of functional groups, which could have implications in recognition, sensing, and separation.

Supplementary Material

Refer to Web version on PubMed Central for supplementary material.

Acknowledgments

We thank NIGMS of the National Institute of Health and the Office of Naval Research for partial support.

References

1. a Fréchet, JMJ.; Tomalia, DA. Dendrimers and Other Dendritic Polymers. John Wiley & Sons; New York: 2001. b Newkome, GR.; Moorefield, CN.; Vögtle, F. Dendrimers and Dendrons: Concepts, Synthesis and Applications. Vol. 2nd Ed.. Wiley-VCH; Weinheim: 2001. c Grayson SM, Fréchet JMJ. Chem. Rev 2001;101:3819. [PubMed: 11740922] d Bosman AW, Janssen HM, Meijer EW. Chem. Rev 1999;99:1665. [PubMed: 11849007] e Moore JS. Acc. Chem. Res 1997;30:402. f Caminade AM, Majoral JP. Acc. Chem. Res 2004;37:341. [PubMed: 15196043] g Balzani V, Campagna S, Denti G, Juris A, Serroni S, Venturi M. Acc. Chem. Res 1998;31:26. h Astruc D, Chardac F. Chem. Rev 2001;101:2991. [PubMed: 11749398] i Majoral JP, Caminade AM. Chem. Rev 1999;99:845. [PubMed: 11749433] j Crespo L, Sanclimens G, Pons M, Giralt E, Royo M, Albericio F. Chem. Rev 2005;105:1663. [PubMed: 15884786] k Zeng F, Zimmerman SC. Chem. Rev 1997;97:1681. [PubMed: 11851463] l Cardona CM, Mendoza S, Kaifer AE. Chem. Soc. Rev 2000;29:37.
2. a Hecht S, Fréchet JMJ. Angew. Chem., Int. Ed 2001;40:74. b Hahn U, Gorka M, Vögtle F, Vicinelli V, Ceroni P, Maestri M, Balzani V. Angew. Chem., Int. Ed 2002;41:3595. c Balzani V, Ceroni P, Maestri M, Vicinelli V. Curr. Opin. Chem. Biol 2003;7:657. [PubMed: 14644173] d Gilat SL, Adronov A, Fréchet JMJ. Angew. Chem., Int. Ed 1999;38:1422. e Devadoss C, Bharathi P, Moore JS. J. Am. Chem. Soc 1996;118:9635–9644. f Stewart GM, Fox MA. J. Am. Chem. Soc 1996;118:4354–60. g Wang S, Hong JW, Bazan GC. Org. Lett 2005;7:1907. [PubMed: 15876016] h Zhou X, Tyson DS, Castellano FN. Angew. Chem., Int. Ed 2000;39:4301. i Halim M, Pillow JNG, Samuel IDW, Burn PL. Adv. Mater 1999;11:371.
3. a Dandliker PJ, Diederich F, Gross M, Knobler CB, Louati A, Sanford EM. Angew. Chem., Int. Ed 1994;33:1739. b Gorman CB, Parkhurst BL, Su WY, Chen K-Y. J. Am. Chem. Soc 1997;119:1141. c Cardona CM, Kaifer AE. J. Am. Chem. Soc 1999;121:9756. d Smith DK, Diederich F. Chem. Eur. J 1998;4:1353. and references therein. e Kaifer AE. Eur. J. Inorg. Chem 2007:5015. f Chow H-F, Chan IYK, Chan DTW, Kwok RWM. Chem.-Eur. J 1996;2:1085.
4. a Albrecht M, Van Koten G. Adv. Mater 1999;11:171. b Bhyrappa P, Young JK, Moore JS, Suslick KS. J. Am. Chem. Soc 1996;118:5708. c Delort E, Darbre T, Reymond J-L. J. Am. Chem. Soc 2004;126:15642. [PubMed: 15571376] d Delort E, Nguyen-Trung N-Q, Darbre T, Reymond J-L. J. Org. Chem 2006;71:4468. [PubMed: 16749776] e Eric Oosterom G, van Haaren RJ, Reek JNH, Kamer PCJ, van Leeuwen PWNM. Chem. Commun 1999:1119. f Jiang D-L, Aida T. Chem. Commun 1996:1523. g Kassube JK, Gade LH. Top. Organomet. Chem 2006;20:61. h Kreiter R, Kleij AW, Gebbink RJMK, van Koten G. Top. Curr. Chem 2001;217:163. i Ribourdouille Y, Engel Gerald D, Richard-Plouet M, Gade Lutz H. Chem. Commun 2003:1228.
5. a Cardona CM, Kaifer AE. J. Am. Chem. Soc 1998;120:4023. b Gorman CB, Smith JC. Acc. Chem. Res 2001;34:60. [PubMed: 11170357] c Bo Z, Rabe JP, Schlüter AD. Angew. Chem., Int. Ed 1999;38:2370. d Hecht S, Fréchet JMJ. Angew. Chem., Int. Ed 2001;40:74. e Oosterom GE, Reek JNH, Kamer PCJ, van Leeuwen PWNM. Angew. Chem., Int. Ed 2001;40:1828. f Larré C, Caminade A-M, Majoral J-P. Angew. Chem., Int. Ed 1997;36:596. g Koper GJM, van Genderen MHP, Elissen-Román C, Baars MWPL, Meijer EW, Borkovec M. J. Am. Chem. Soc 1997;119:6512. h Yamamoto K, Higuchi M, Shiki S, Tsuruta M, Chiba H. Nature 2002;415:509. [PubMed: 11823855] i Krishnamoorthy K, Dasari RR, Nantalaksakul A, Thayumanavan S. Chem. Commun 2007:739.
6. a Hawker CJ, Wooley KL, Fréchet JMJ. J. Am. Chem. Soc 1993;115:4375. b Devadoss C, Bharathi P, Moore JS. Angew. Chem., Int. Ed 1997;36:1633. c Campagna S, Denti G, Serroni S, Juris A, Venturi M, Ricevuto V, Balzani V. Chem. Eur. J 1995;1:211. d Jiang D-L, Aida T. Nature 1997;388:454. e Brewis M, Clarkson GJ, Goddard V, Helliwell M, Holder AM, McKeown NB. Angew. Chem., Int. Ed 1998;37:1092. f Nlate S, Nieto Y, Blais J-C, Ruiz J, Astruc D. Chem. Eur. J 2002;8:171. g Cuadrado I, Casado CM, Alonso B, Moran M, Losada J, Belsky V. J. Am. Chem. Soc 1997;119:7613. h Newkome GR, Güther R, Moorefield CN, Cardullo F, Echegoyen L, E. Cordero P, Luftmann H. Angew. Chem., Int. Ed 1995;34:2023. i Stone DL, Smith DK, McGrail PT. J. Am. Chem. Soc 2002;124:856. [PubMed: 11817961] j Casado CM, Cuadrado I, Moran M, Alonso B, Garcia B, Gonzalez B, Losada J. Coord. Chem. Rev 1999;185-186:53. k Castro R, Cuadrado I, Alonso B, Casado CM, Moran M, Kaifer AE. J. Am. Chem. Soc 1997;119:5760. l Takada K, Diaz DJ, Abruna HD, Cuadrado I, Casado C, Alonso B, Moran M, Losada J. J. Am. Chem. Soc 1997;119:10763.
7. Sivanandan K, Aathimanikandan SV, Arges CG, Bardeen CJ, Thayumanavan S. J. Am. Chem. Soc 2005;127:2020. [PubMed: 15713060]

8. a Sivanandan K, Vutukuri D, Thayumanavan S. Org. Lett 2002;4:3751. [PubMed: 12375935] b Sivanandan K, Sandanaraj BS, Thayumanavan S. J. Org. Chem 2004;69:2937. [PubMed: 15104429] c Nantalaksakul A, Dasari RR, Ahn T-S, Al-Kaysi R, Bardeen CJ, Thayumanavan S. Org. Lett 2006;8:2981. [PubMed: 16805532] d Zhang W, Nowlan DT III, Thomson LM, Lackowski WM, Simanek EE. J. Am. Chem. Soc 2001;123:8914. [PubMed: 11552798] e Newkome GR, Kim HJ, Moorefield CN, Maddi H, Yoo K-S. Macromolecules 2003;36:4345. f Woller EK, Walter ED, Morgan JR, Singel DJ, Cloninger MJ. J. Am. Chem. Soc 2003;125:8820. [PubMed: 12862477] g Hawker CJ, Fréchet JMJ. Macromolecules 1990;23:4726. h Hawker CJ, Fréchet JMJ. J. Am. Chem. Soc 1992;114:8405.

9. a Casado CM, Gonzalez B, Cuadrado I, Alonso B, Moran M, Losada J. Angew. Chem., Int. Ed 2000;39:2135. b Chandrasekhar V, Andavan GTS, Nagendran S, Krishnan V, Azhakar R, Butcher RJ. Organometallics 2003;22:976–986. c Koellner C, Pugin B, Togni A. J. Am. Chem. Soc 1998;120:10274. d Salmon A, Jutzi P. J. Organomet. Chem 2001;637-639:595. e Sengupta S. Tetrahedron Lett 2003;44:7281. f Valerio C, Fillaut J-L, Ruiz J, Guittard J, Blais J-C, Astruc D. J. Am. Chem. Soc 1997;119:2588.

10. a Vutukuri DR, Basu S, Thayumanavan S. J. Am. Chem. Soc 2004;126:15636. [PubMed: 15571373] b Savariar EN, Aathimanikandan SV, Thayumanavan S. J. Am. Chem. Soc 2006;128:16224. [PubMed: 17165775] c Bharathi P, Zhao H, Thayumanavan S. Org. Lett 2001;3:1961. [PubMed: 11405755]

11. a Rostovtsev VV, Green LG, Fokin VV, Sharpless KB. Angew. Chem., Int. Ed 2002;41:2596. For the review on click chemistry, see: b Lutz J-F. Angew. Chem., Int. Ed 2007;46:1018. For the utilization of click chemistry in dendrimers, see: c Wu P, Feldman AK, Nugent AK, Hawker CJ, Scheel A, Voit B, Pyun J, Fréchet JMJ, Sharpless KB, Fokin VV. Angew. Chem., Int. Ed 2004;43:3928.

12. See supporting information for details.

13. Mirkin MV, Bard AJ. Anal. Chem 1992;64:2293.

14. Podkoscielny D, Hooley RJ, Rebek J Jr, Kaifer AE. Org. Lett 2008;10:2865. [PubMed: 18537255]

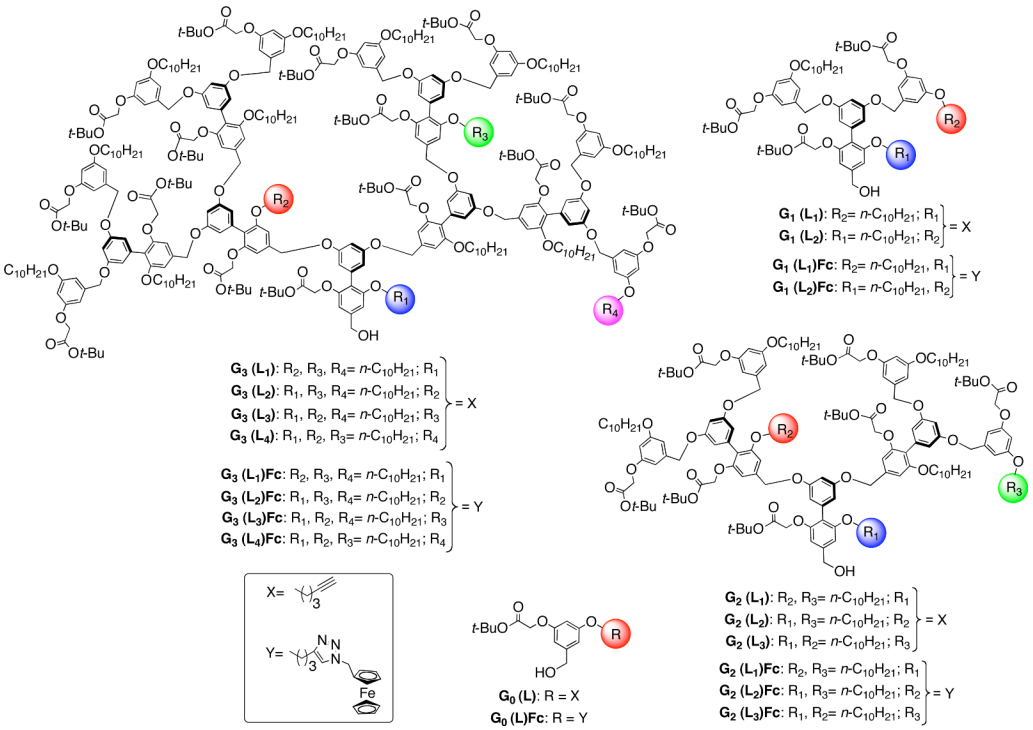

Chart 1.
Structures of functionalized dendrons

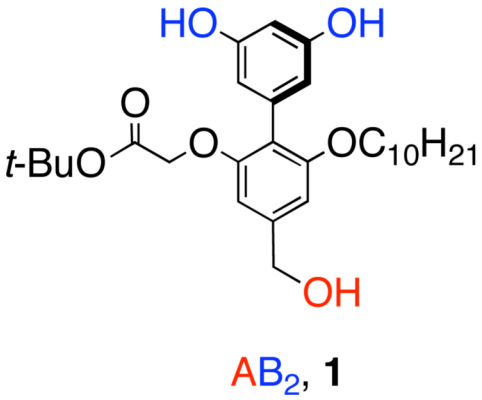

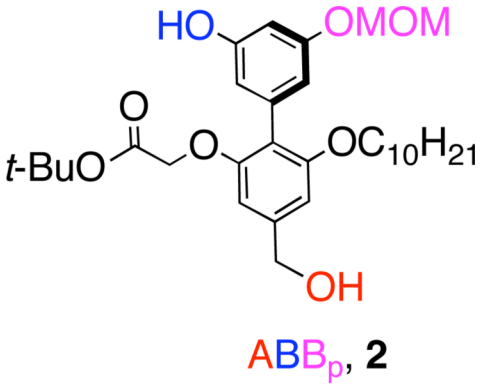

Chart 2.
Structures AB_2 and ABB_p monomers

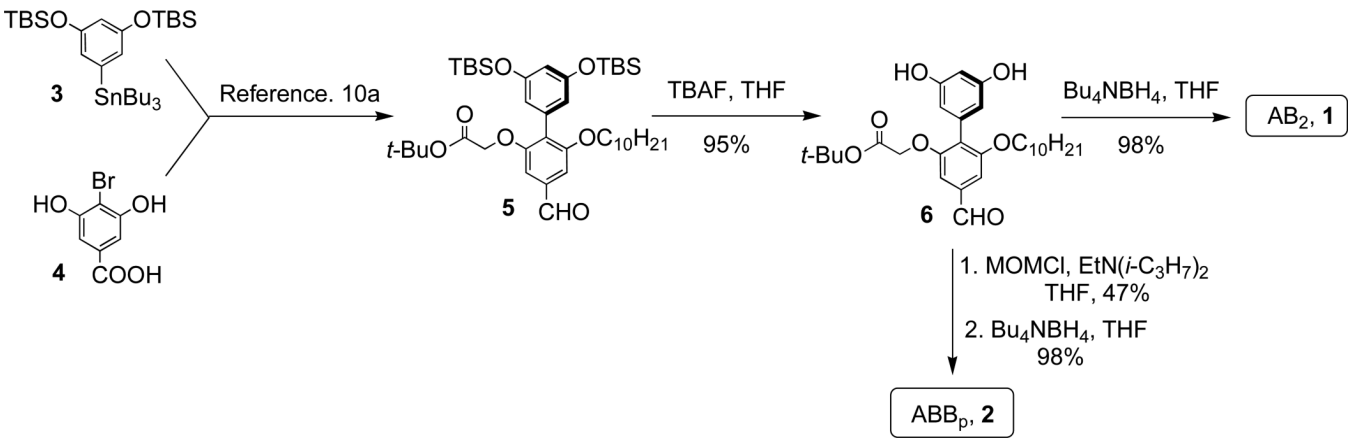

Scheme 1.
Synthesis of ABB_p and AB_2 monomers

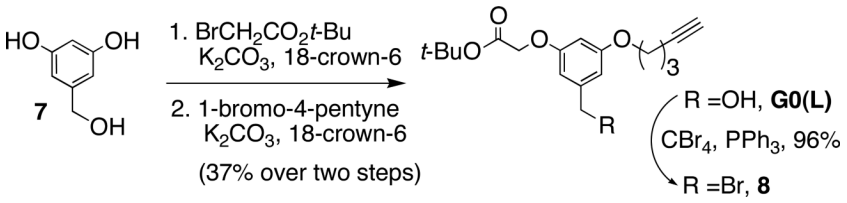

Scheme 2.
Synthesis of **G0(L)** dendron and its bromide

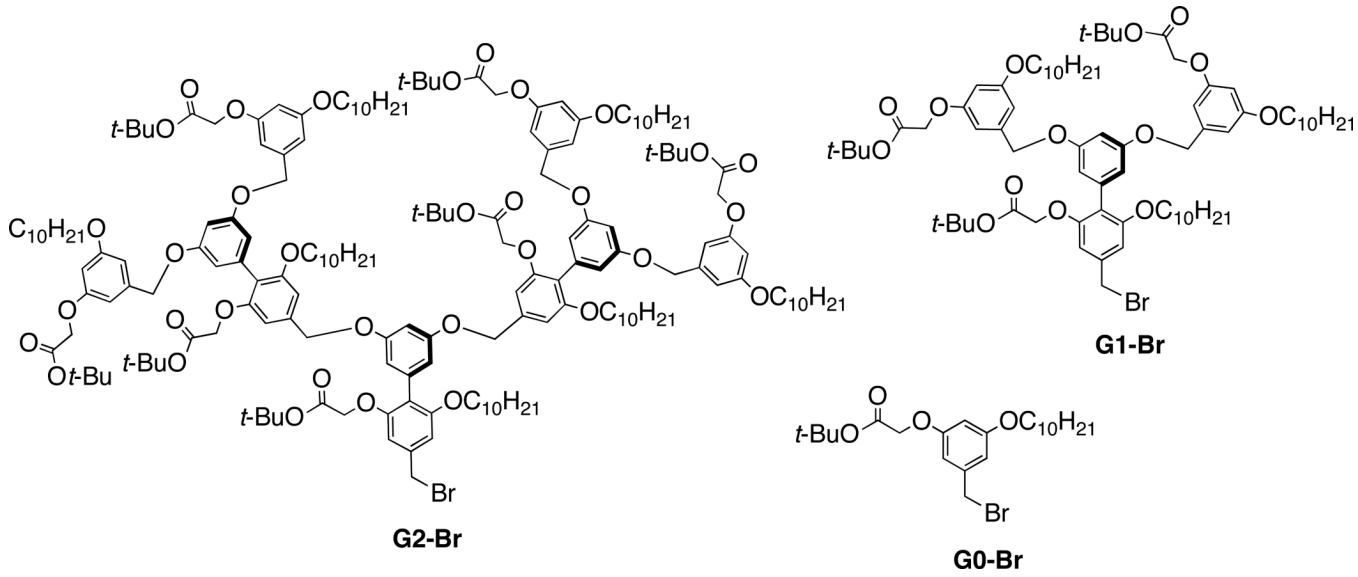

Chart 3.
Structures of **G0-Br**, **G1-Br** and **G2-Br**

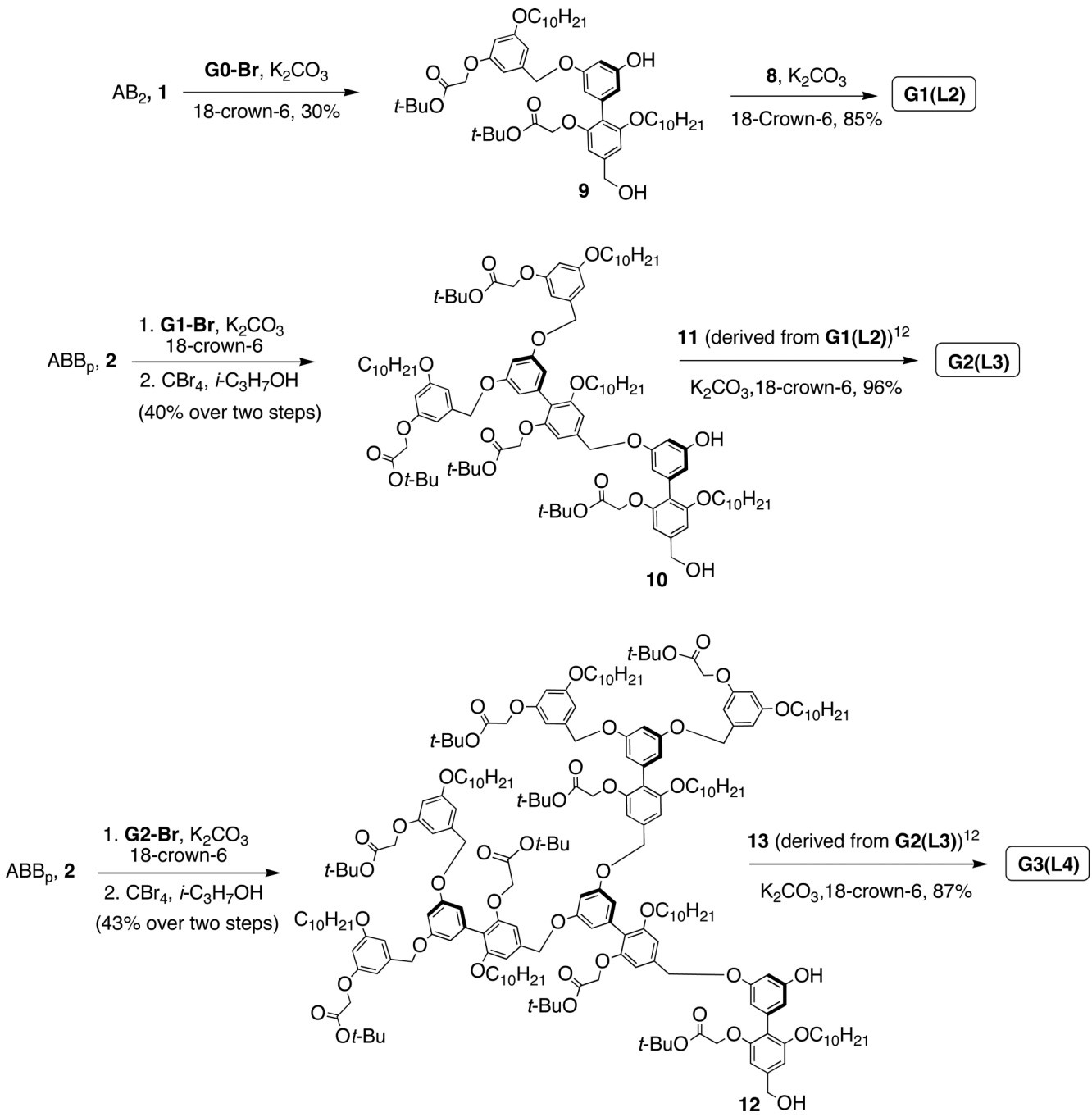

Scheme 3.
Synthesis of peripherally functionalized dendrons

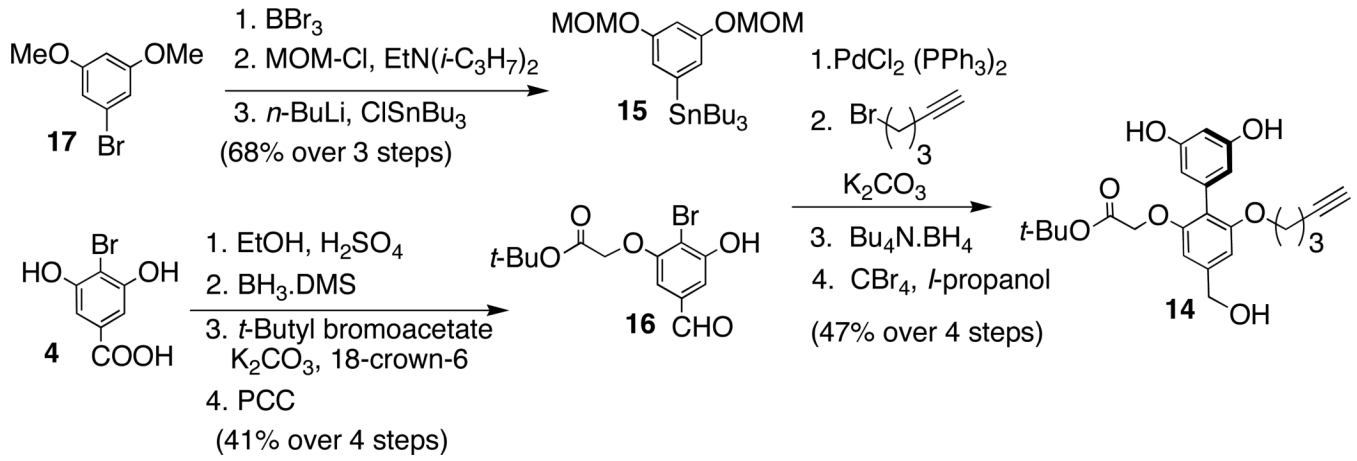

Scheme 4.
Synthesis of acetylene-functionalized monomer

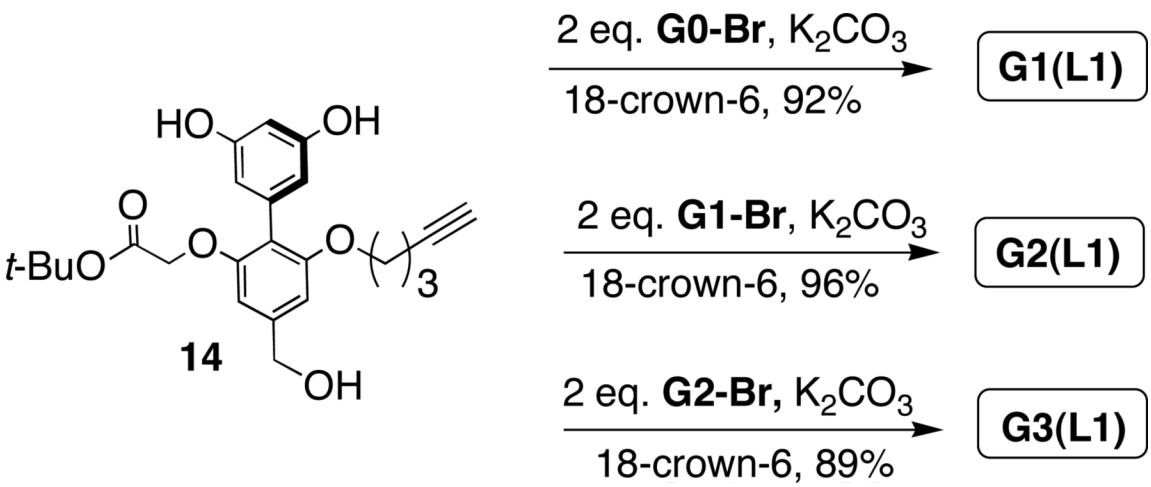

Scheme 5.
Synthesis of functionalized dendrons at the focal point

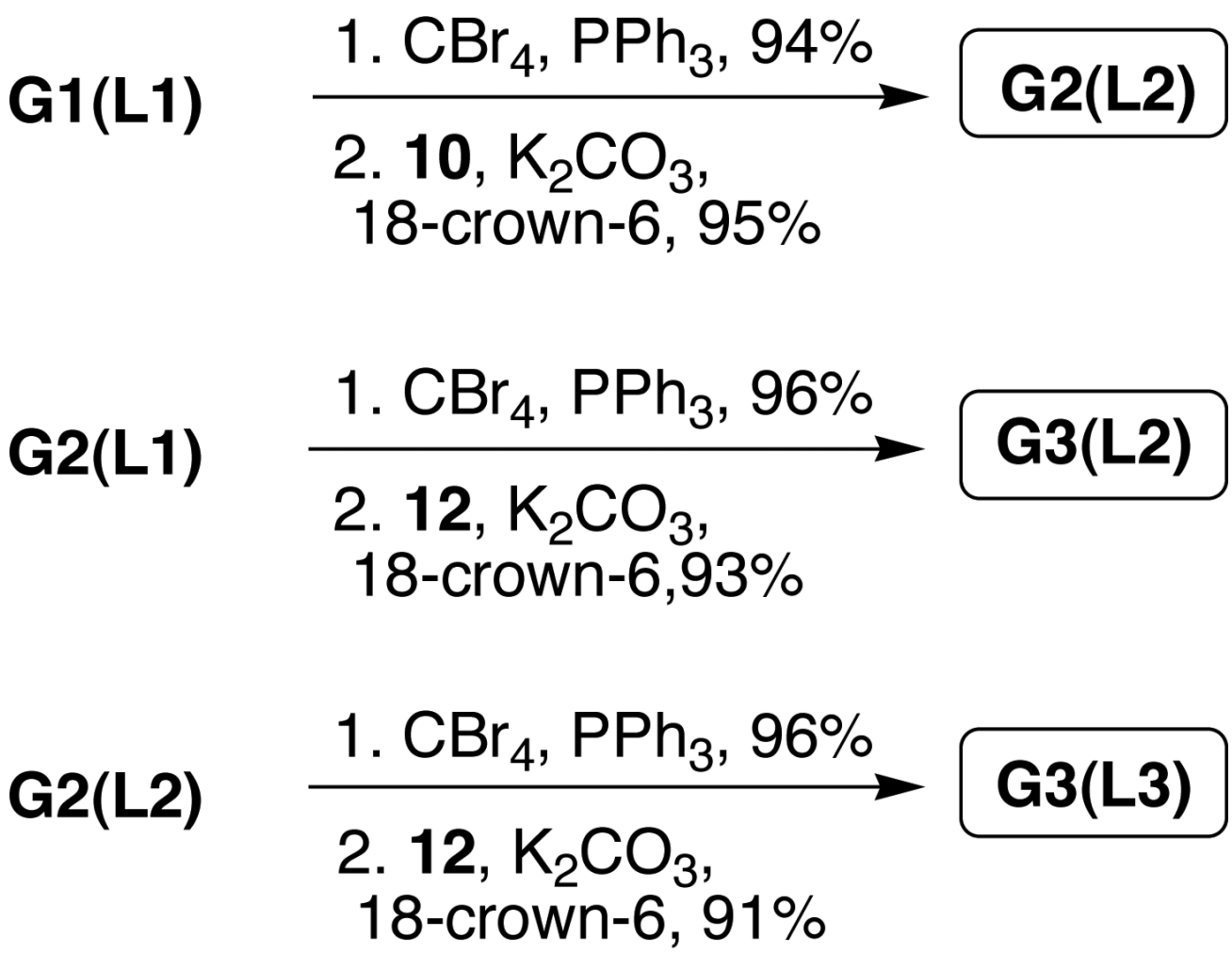

Scheme 6.
Synthesis of intermediate layer functionalized dendrons

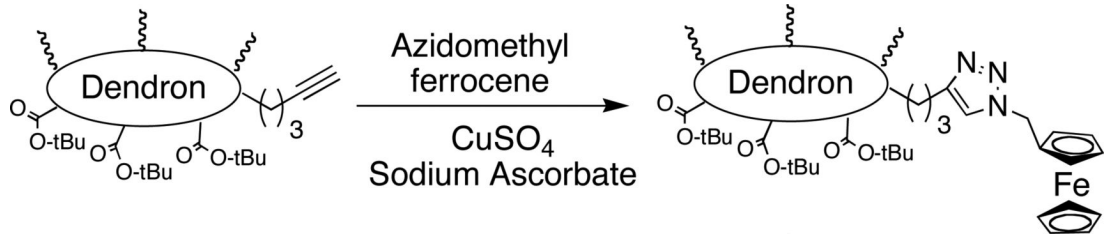

Scheme 7.
Incorporation of ferrocene into the alkyne containing dendrons through click chemistry

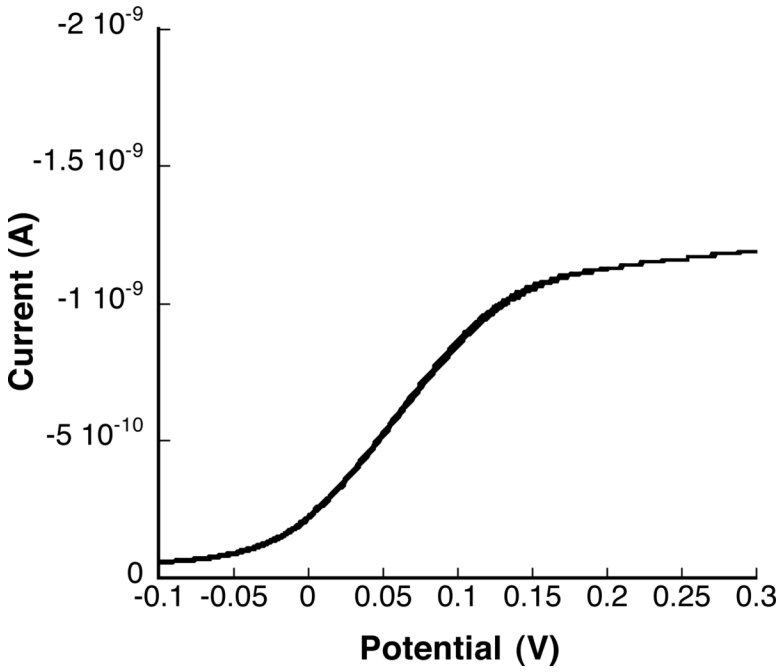

Figure 1.
Steady state cyclic voltammogram of **G3(L2)Fc** in DMF

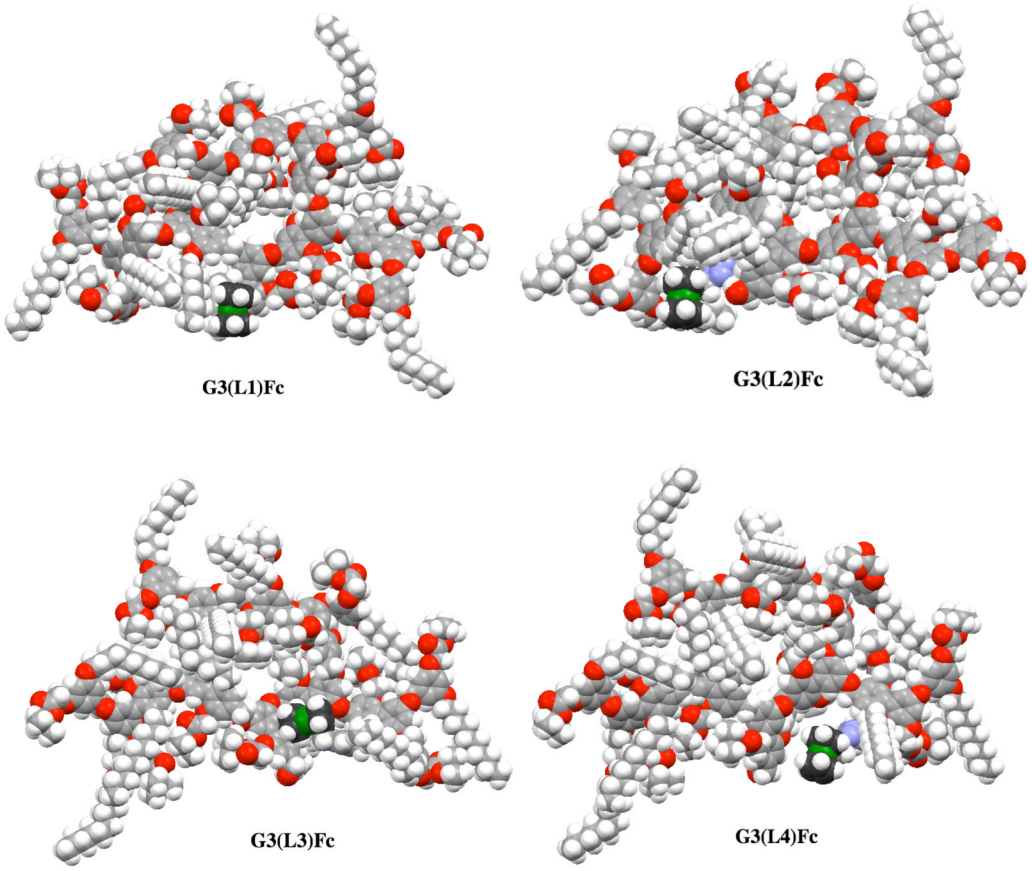

Figure 2.
Energy minimized structures of G3 dendrons with ferrocene at different locations (ferrocene is shown in black and green colors)

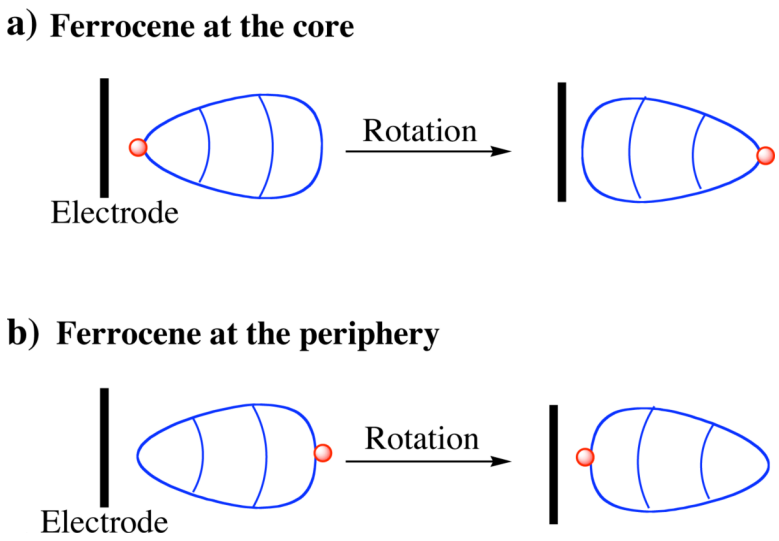

Figure 3.
Orientation of G3 dendron towards the electrode due to its free rotation

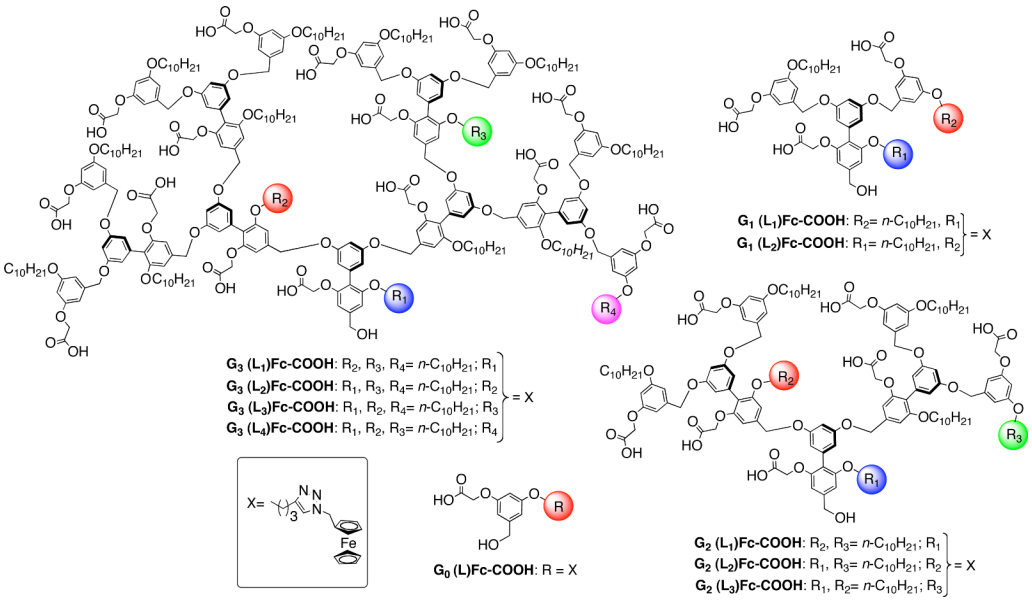

Chart 4.
Structures of ferrocene incorporated amphiphilic dendrons

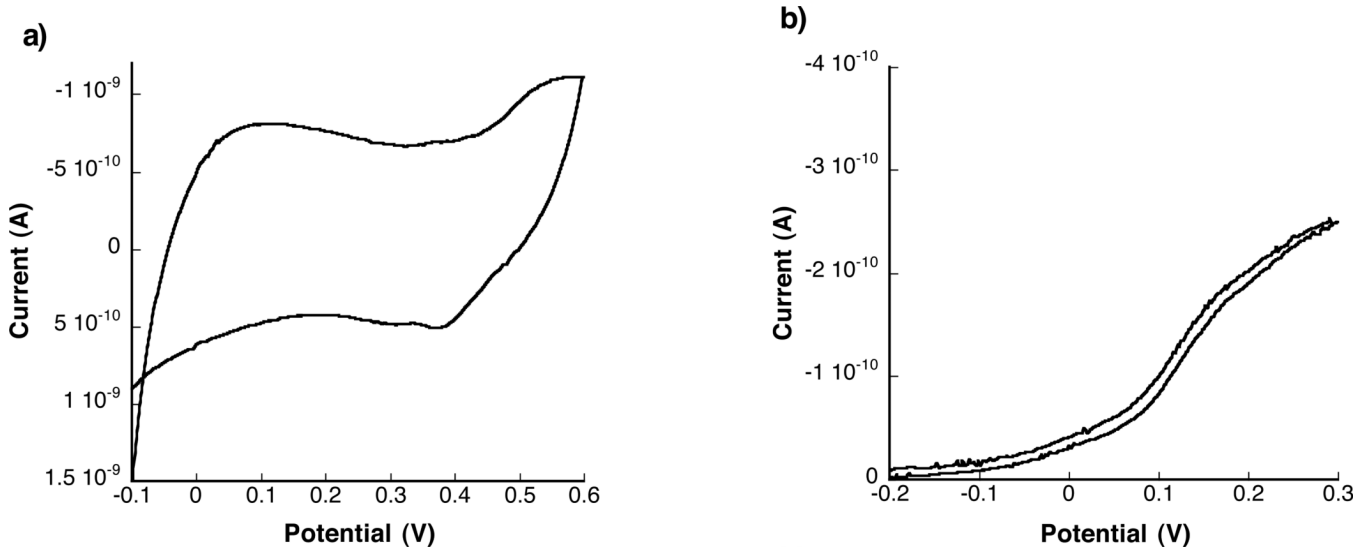

Figure 4.
Cyclic voltammogram of (a) **G3(L1)Fc-COOH** in water and (b) **G3(L1)Fc-COOH** in DMF

Table 1

Electrochemical data for Non-amphiphilic dendrons in DMF

Dendrons	$E_{1/2}$	D_0 (cm^2/s)	k^0 (cm/s)
G0(L)Fc	103	5.1×10^{-6}	1.9×10^{-4}
G1(L1)Fc	118	2.0×10^{-6}	1.8×10^{-4}
G1(L2)Fc	114	2.0×10^{-6}	3.1×10^{-4}
G2(L1)Fc	113	1.0×10^{-6}	1.5×10^{-4}
G2(L2)Fc	69	1.0×10^{-6}	1.9×10^{-4}
G2(L3)Fc	117	1.0×10^{-6}	1.4×10^{-4}
G3(L1)Fc	101	1.1×10^{-6}	1.4×10^{-4}
G3(L2)Fc	60	1.1×10^{-6}	1.5×10^{-4}
G3(L3)Fc	68	1.1×10^{-6}	1.8×10^{-4}
G3(L4)Fc	120	1.1×10^{-6}	1.7×10^{-4}